시스템 동정을 통한 구조물의 결함 탐지
Structural Damage Detection through System Identification

고봉환† · S. Nagarajaiah* · M.Q. Phan**
Bong-Hwan Koh, S. Nagarajaiah, and M.Q. Phan

Key Words : System identification (시스템 동정), Damage detection (결함 탐지), Kronecker product (크로네커 곱).

ABSTRACT

This paper presents an experimental investigation of a recently developed Kronecker Product (KP) method to determine the type, location, and intensity of structural damage from an identified state-space model of the system. Although this inverse problem appears to be highly nonlinear, the system mass, stiffness, and damping matrices are identified through a series of transformations, and with the aid of the Kronecker product, only linear operations are involved in the process. Since a state-space model can be identified directly from input-output data, an initial finite element model and/or model updating are not required. The test structure is a two-degree-of-freedom torsional system in which mass and stiffness are arbitrarily adjustable to simulate various conditions of structural damage. This simple apparatus demonstrates the capability of the damage detection method by not only identifying the location and the extent of the damage, but also differentiating the nature of the damage. The potential applicability of the KP method for structural damage identification is confirmed by laboratory test.

1. Introduction

The research on the realization of state-space model from input-output data has been well developed for the last few decades. A standard system identification algorithm such as OKID-ERA [1,2] determines a minimally realized state-space model from observer Markov parameters and truncation of a Hankel matrix. However rearranging a state-space model into a second-order form such as mass, stiffness, and damping matrices is non-trivial because typically a realized state-space model is not in physical coordinates. There have been several research efforts trying to extract second-order mechanical system matrices from identified state-space model. Alvin and Park [3] developed a transformation algorithm using the McMillan normal form realization. The study also includes other variants of the method that can estimate normal mode from non-proportional damping through pseudo-normal mode basis. Tseng *et. al.* [4] investigated an algorithm that can also deal with gyroscopic systems with repeated undamped modal frequencies. Angelis *et. al.* [5] proposed a more generalized technique that relaxes the constraints on the number of sensors/actuator and co-location requirement. However, all of these studies need an intermediate nonlinear step of solving eigenvalue problems. Recently, Phan and Longman [6] developed a linear solution for extracting system parameters in physical coordinates via the properties of Kronecker product and stack operation. First, a state-space model is identified from input-output data by any state-space system identification technique such as OKID-ERA. From such an identified state-space model, structural properties, i.e., stiffness, mass, and damping matrices can be extracted from a series of linear transformations.

Previously, Ray and Koh [7] investigated a damage detection problem in torsional system, given empirical correlation between feedback control gain and sensitivity of modal frequencies. Experiment results proved that modal sensitivity of structural damage in torsional system could be significantly enhanced through sensitivity enhancing control (SEC). However, their approach, like all other modal-based damage detection methods, requires the information of modal frequencies of the test structure. Modal frequency is a global property of dynamic system and sensitive to both mass and stiffness variations. In general, observation of modal frequency change alone is insufficient for identifying the type of damage (i.e., mass or stiffness).

This paper presents an experimental demonstration of Kronecker Product (KP) method [6]. The technique directly applies to damage detection problem by comparing the reconstructed structural parameters such as mass and stiffness before and after the occurrence of damage. The strength of this approach lies in a successful identification of damage presence, location, and type, without any priori knowledge of the FE model of the structure. First, the mathematical formulation of KP method is briefly explained. Secondly, the description of experimental procedure and test setup are

† 책임저자; 동국대학교 기계공학과, 정회원
E-mail : bkoh@dongguk.edu
Tel : (02) 2260-8591, Fax : (02) 2263-9379
* Dept. of Civil Engineering, Rice University, USA
** Thayer School of Engineering, Dartmouth College, USA

presented. The test-bed in this study is a two-degree-of-freedom torsional system. The method does not require modal frequencies or a baseline finite element model. To introduce different types of damage conditions, mass and stiffness of the system are systematically perturbed. Finally, test results are presented and discussed in terms of damage localization and classification of damage type. This experimental demonstration should be considered as a preliminary step in series of efforts for implementing a system identification algorithm into the development of structural damage identification technique for more complicated structures. The same experiment data, i.e., input-output time history of the torsional system in reference [7] is used in this study.

2. Kronecker Product Method

Although the reference [6] provides a detailed derivation of KP method, for the sake of completeness, a brief summary is provided for the case of having a full set of displacement measurement in this section. Consider a spatially discrete system having n physical coordinates $w(t)$ and r inputs $u(t)$

$$\mathsf{M}\ddot{w}(t)+\Theta\dot{w}(t)+\mathsf{K}w(t)=\mathsf{B}u(t) \tag{1}$$

where M, Θ, and K are mass, damping, and stiffness matrices, respectively. The $\mathsf{B}(n\times r)$ is the input influence matrix. The second-order equation of motion can be rewritten in a state-space format with its physical coordinate intact as

$$\begin{aligned}\dot{x}(t)&=Ax(t)+Bu(t)\\ y(t)&=Cx(t)+Du(t)\end{aligned} \tag{2}$$

$$\dot{x}(t)=\begin{bmatrix}w(t)\\ \dot{w}(t)\end{bmatrix},\quad A=\begin{bmatrix}0_{n\times n} & I_{n\times n}\\ -\mathrm{H}_1 & -\mathrm{H}_2\end{bmatrix},\quad B=\begin{bmatrix}0_{n\times r}\\ \mathrm{H}_3\end{bmatrix} \tag{3}$$

Here, partitions holding M, Θ, and K can be expressed as

$$\mathrm{H}_1=\mathsf{M}^{-1}\mathsf{K},\quad \mathrm{H}_2=\mathsf{M}^{-1}\Theta,\quad \mathrm{H}_3=\mathsf{M}^{-1}\mathsf{B} \tag{4}$$

If we have a full set of displacement measurements (which is the case for this experiment),

$$C=[I_{n\times n}\quad 0_{n\times n}],\quad D=0_{n\times r} \tag{5}$$

Given $\mathrm{H}_{i=1\ldots3}$ in physical coordinates, structural parameters M,Θ, and K can be extracted from the Kronecker product and stack operator techniques presented in Section 2.2.

2.1 Transforming Physical Coordinates

Unfortunately, a realized state-space model is not necessarily in the physical coordinates given in Eq. (3) and (4). Then the first step in extracting $\mathsf{M},\Theta,\mathsf{K}$ is to transform a realized state-space model into a physical coordinate system. Here a transformation matrix is developed that will transform any realized state-space model (A_r,B_r,C_r) into the physical coordinates of (A,B,C). We review the case where full set of displacement measurements is available. Other cases for velocity, acceleration, and mixed measurements are explained in the reference [6]. In deriving this transformation matrix, a similarity transformation matrix Q is used.

$$\begin{aligned}\tilde{A}&=Q(A_r)Q^{-1}\\ \tilde{B}&=Q(B_r)\\ \tilde{C}&=(C_r)Q^{-1}=[I_{n\times n}\quad 0_{n\times n}]=C\end{aligned} \tag{6}$$

where,

$$Q=\begin{bmatrix}C_r\\ \overline{Q}\end{bmatrix} \tag{7}$$

here, $\overline{Q}$ is any nonsingular matrix. This intermediate step is purely to transform C_r into C. Another similarity transformation T is needed to transform $(\tilde{A},\tilde{B})$ into (A,B) without modifying C which is already transformed correctly by Q. Accordingly, the transformation matrix T should satisfy

$$\begin{aligned}A&=T(\tilde{A})T^{-1}\\ B&=T(\tilde{B})\\ \tilde{C}&=(\tilde{C})T^{-1}\end{aligned} \tag{8}$$

For further development, T, A, $\tilde{A}$, and B are partitioned as

$$\begin{aligned}&T=\begin{bmatrix}T_{11} & T_{12}\\ T_{21} & T_{22}\end{bmatrix},\quad A=\begin{bmatrix}0 & I\\ A_{21} & A_{22}\end{bmatrix},\\ &\tilde{A}=\begin{bmatrix}(\tilde{A})_{11} & (\tilde{A})_{12}\\ (\tilde{A})_{21} & (\tilde{A})_{22}\end{bmatrix},\quad B=\begin{bmatrix}B_1\\ B_2\end{bmatrix}\end{aligned} \tag{9}$$

Note that the transformed matrices $(\tilde{A},\tilde{B})$ belong to an intermediate step between a realized state-space model and a state-space model in physical coordinate. Here, another condition is imposed to T that will preserve $\tilde{C}$,

$$[I\quad 0]\begin{bmatrix}T_{11} & T_{12}\\ T_{21} & T_{22}\end{bmatrix}=[I\quad 0] \tag{10}$$

In order to satisfy Eq. (10), $T_{11}=I$ and $T_{12}=0$. From Eq. (8), it is obvious that

$$\begin{bmatrix} 0 & I \\ A_{21} & A_{22} \end{bmatrix}\begin{bmatrix} I & 0 \\ T_{21} & T_{22} \end{bmatrix} = \begin{bmatrix} I & 0 \\ T_{21} & T_{22} \end{bmatrix}\begin{bmatrix} (\tilde{A})_{11} & (\tilde{A})_{12} \\ (\tilde{A})_{21} & (\tilde{A})_{22} \end{bmatrix} \tag{11}$$

which produces $T_{21} = (\tilde{A})_{11}$, and $T_{22} = (\tilde{A})_{12}$. Thus, the transformation matrix T that transforms $(\tilde{A},\tilde{B},\tilde{C})$ to (A,B,C) in physical coordinate becomes

$$T = \begin{bmatrix} I & 0 \\ (\tilde{A})_{11} & (\tilde{A})_{12} \end{bmatrix} \tag{12}$$

After the transformation is completed, it is easy to find $\mathrm{H}_{i=1...3}$ that are simply the partitions of A, B as

$$\mathrm{H}_1 = -A_{21},\ \mathrm{H}_2 = -A_{22},\ \mathrm{H}_3 = B_2 \tag{13}$$

2.2 Extracting System Matrices

Having rearranged a realized state-space model (A_r,B_r,C_r) into a physical coordinate system (A,B,C) through two consecutive transformations (Q,T), all partitions $\mathrm{H}_{i=1...3}$ are defined. Next, physical parameters of second-order dynamical system (M, Θ, and K) can be simultaneously recovered with the aid of the Kronecker product and the stack operator. The following identity is used.

$$(ABC)^S = (C^T \otimes A)B^S \tag{14}$$

In order to maintain the symmetry of M, K, and possibly Θ, two additional equations should be considered as

$$\begin{aligned} \mathsf{M}\mathrm{H}_1 &= \mathrm{H}_1^{\mathrm{T}}\mathsf{M} \\ \mathsf{M}\mathrm{H}_2 &= \mathrm{H}_2^{\mathrm{T}}\mathsf{M} \end{aligned} \tag{15}$$

Imposing symmetry conditions in Eq. (15) plays a key role in finding M, K, and Θ because knowing $\mathrm{H}_{i=1...3}$ is not enough to solve Eq. (5). Also, note that the symmetry condition of the damping matrix (Θ) is not needed for the case of non-symmetric damping. Combining Eq. (5) and (15), we have the following set of linear equations,

$$\begin{aligned} \mathsf{K}^S &= (\mathrm{H}_1^{\mathrm{T}} \otimes I)\mathsf{M}^S \\ \Theta^S &= (\mathrm{H}_2^{\mathrm{T}} \otimes I)\mathsf{M}^S \\ \mathsf{B}^S &= (\mathrm{H}_3^{\mathrm{T}} \otimes I)\mathsf{M}^S \\ (\mathrm{H}_1^{\mathrm{T}} \otimes I)\mathsf{M}^S &= (I \otimes \mathrm{H}_1^{\mathrm{T}})\mathsf{M}^S \\ (\mathrm{H}_2^{\mathrm{T}} \otimes I)\mathsf{M}^S &= (I \otimes \mathrm{H}_2^{\mathrm{T}})\mathsf{M}^S \end{aligned} \tag{16}$$

Thus, the elements of mass, stiffness, and damping matrices are determined by solving a linear equation,

$$RP = S \tag{17}$$

where

$$R = \begin{bmatrix} \mathrm{H}_1^{\mathrm{T}} \otimes I & 0 & -I \\ \mathrm{H}_2^{\mathrm{T}} \otimes I & -I & 0 \\ \mathrm{H}_3^{\mathrm{T}} \otimes I & 0 & 0 \\ (\mathrm{H}_1^{\mathrm{T}} \otimes I) - (I \otimes \mathrm{H}_1^{\mathrm{T}}) & 0 & 0 \\ (\mathrm{H}_2^{\mathrm{T}} \otimes I) - (I \otimes \mathrm{H}_2^{\mathrm{T}}) & 0 & 0 \end{bmatrix},\ P = \begin{bmatrix} \mathsf{M}^S \\ \Theta^S \\ \mathsf{K}^S \end{bmatrix},$$
$$S = \begin{bmatrix} 0 \\ 0 \\ \mathsf{B}^S \\ 0 \\ 0 \end{bmatrix} \tag{18}$$

As long as R is full (column) rank, the symmetry condition on the damping matrix is not needed to solve for the elements of M, K, and Θ because Eq. (18) actually contains more equations then the minimum needed.

3. Experimental Procedure

3.1 Description of Torsional System

As described in reference [7,8], originally the torsional system has three inertia disks connected by two torsionally flexible rods or preferably called torsional springs [9]. By clamping the top disk to the body frame, a 2-DOF spring-mass-damper system of fixed-free boundary condition can be modeled as shown in Figure 1 The brushless servo motor, as an input force, drives the shaft that is linked to the bottom disk by torque $T(t)$. The angular displacement (θ) of each disk is measured from optical encoder attached through a rigid belt and pulley. Therefore, the test structure in this study has a single torque input and two angular displacement outputs.

As shown in Figure 1, the stiffness of the torsional spring or rod and the inertia of disk are defined as k_i and J_i, respectively. Placing a stiffener-type clamp at the center of a torsional spring rod creates stiffness damage. This clamp locally resists the rotation of the rod so that the stiffness of torsional spring is increased by a certain degree. The degree of stiffening is nonlinear function of the contact force and the area between the spring rod and the stiffening plate. Mass damage is also easily implemented by relocating mass blocks on each disk. As shown in Figure 1, each disk has four mass blocks and adjustable slots. The inertia of the disk can be roughly estimated from calculating mass of four blocks and their distance to the centerline (a). Thus, both stiffness and inertia of torsional system can be readily perturbed to imitate different types of damage conditions.

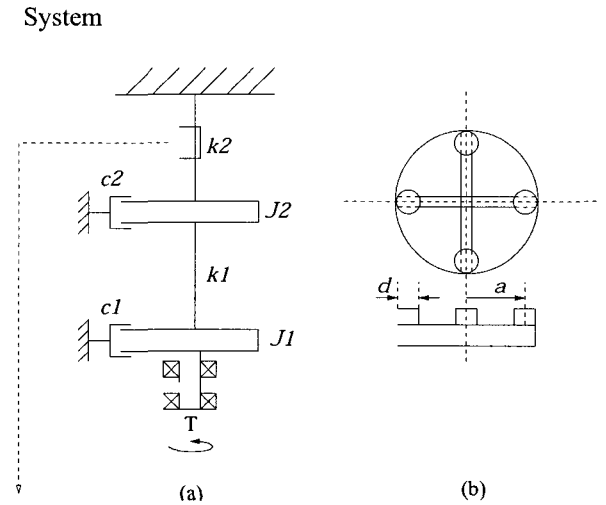

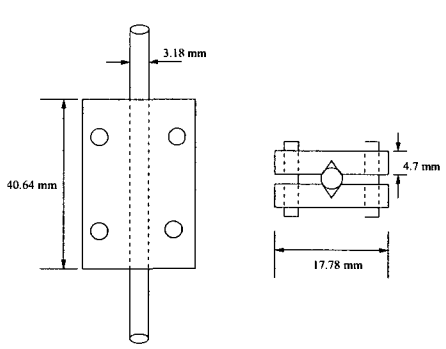

Figure 1. Schematics of 2-DOF torsional system: assembly and stiffener patch for stiffness damage.

3.2 Identification of State-Space Model and Structural Parameters

A Gaussian random noise input to the servo motor excites the torsional system for 60 seconds having sampling time of 0.01 second. Also, dSPACE software has been used for data acquisition. Then, state-space system matrices are sought from the input/output time history data using the OKID-ERA. The final order of the identified model has been reduced to four ($n=4$) through the singular value spectrum of the Hankel matrix. Having determined the minimal state-space model, the stiffness and mass matrices of the system are going to be extracted through KP method. Note that this transformation requires the number of measurement outputs to be equal to the DOFs of second-order model: a condition that is satisfied by encoder for measuring rotational angle at each disk. In other words, the number of measurements determines the size of stiffness and mass matrices.

To represent the dynamics of torsional system, the friction caused from support bearings is idealized to viscous damping (c_i)on each disk. Thus, the equation of motion is

$$\mathsf{J}\ddot{\theta}(t)+\Theta\dot{\theta}(t)+\mathsf{K}\theta(t)=\mathsf{B}u(t) \qquad (19)$$

where J,Θ , and K are mass moment of inertia, damping, and stiffness matrices, respectively:

$$\mathsf{J}=\begin{bmatrix}J_1 & 0\\ 0 & J_2\end{bmatrix},\Theta=\begin{bmatrix}c_1 & 0\\ 0 & c_2\end{bmatrix},\mathsf{K}=\begin{bmatrix}k_1 & -k_1\\ -k_1 & k_1+k_2\end{bmatrix} \qquad (20)$$

Here, input $\mathsf{B}u(t)$ represents a torque, $T(t)$, applied on disk 1 from the servo motor. $\theta(t)=[\theta_1 \;\; \theta_2]^T$ are angular positions of lower and upper disk in Figure 1, respectively. Transforming this into state-space form,

$$\dot{x}=Ax+Bu \qquad (21)$$

where,

$$A=\begin{bmatrix}0 & I\\ -\mathsf{J}^{-1}\mathsf{K} & -\mathsf{J}^{-1}\Theta\end{bmatrix},\; B=\begin{bmatrix}0\\ \mathsf{J}^{-1}\mathsf{B}\end{bmatrix} \qquad (22)$$

and the state is $x=[\theta \;\; \dot{\theta}]^T$. Since, a state-space model (A_r,B_r,C_r) is identified from OKID-ERA, discrete second-order system matrices $(\mathsf{J},\Theta,\mathsf{K})$ are now to be reconstructed by KP method.

4. Damage Cases and Experiment Results

In total, nine different damage cases are investigated. The first three belong to mass damage, i.e., two for mass change on each individual disk and the other one for dual damage on both disks. Here, mass damage is created by moving four mass blocks (4×0.5kg) by $10mm$ toward the center of the disk so that the total inertia for each disk is reduced by approximately 18%. Similar to mass damage, three different stiffness damages are generated, i.e., two cases for each individual torsional spring and the other one for dual damages on both springs. In case of stiffness damage, unlike mass, the true magnitude of stiffness change is not known *a priori*: as it depends on nonlinear contact characteristics between the clamp and the rod. Finally, the last three cases consider a group of mixed type damages such as simultaneously occurred damages on both spring rod and disk. This mixed type damage will illustrate the advantage of the proposed method over other modal-based damage detection approaches that only use modal frequency change.

Figure 2 illustrates identified stiffness and mass parameters of the torsional system for healthy and six different damage cases: (*S1*) stiffness damage on spring 1 (k_1), (S2) stiffness damage on spring 2 (k_2), and (*S12*) for dual damages on both springs.

Likewise mass damage on the disk is denoted as *J1*, *J2*, and *J12*. The individual experiment of healthy and damage case has been repeated for 10 times.

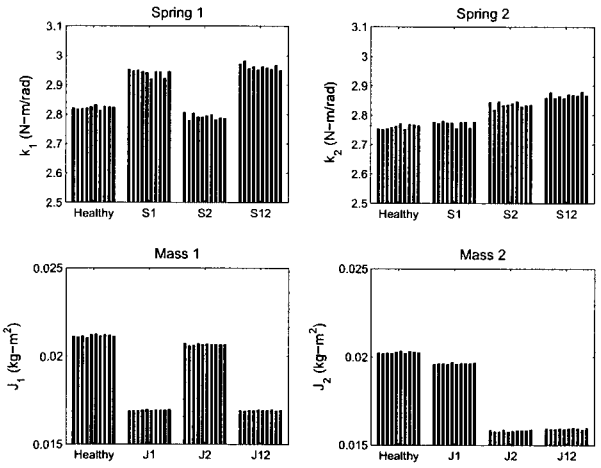

Figure 2. Experimentally identified stiffness and mass moment of inertia for healthy and six different damage cases: *S1*, *S2*, *S12*, *J1*, *J2*, and *J12*.

The height of bar indicates identified value of system parameters: the stiffness of spring and mass inertia of disk. It is obvious from the figure that stiffness changes are observed between healthy and each damage case. Since stiffness damage in this experiment is caused by stiffener patch, spring constants are actually increased compared to healthy cases. The first plot in the figure (*Spring 1*), clearly shows the stiffness increment on the damage cases *S1* and *S12* compared to *Healthy* and *S2*. Likewise, in case of *Spring 2*, damage *S2* and *S12* get higher spring constant values than those of *Healthy* and *S1* cases, which clearly indicate a distinction between damaged and healthy state. Especially, differences between healthy and damaged states of mass (*Mass 1* and *Mass 2*) are more significant than stiffness case. Note that mass damage produces consistent mass reduction ratio of 20%, which is very close to the true reduction of mass moment of inertia (18%). In general, identifying mass change is more accurate than identifying stiffness change. From the perspective of experiment, implementing mass perturbation on the disk is easier than increasing stiffness of the spring. Also, attaching stiffener may produce a similar effect of nonlinear damping to the whole system.

Table 1 summarizes the mean values of identified stiffness, mass, and damping parameters for all cases. Figure 3 presents identification results for mixed-type damage cases. Here, it is considered that two different types of damages, i.e., stiffness and mass damages, are simultaneously occurred. For example, the damage case *S2J1* denotes stiffness damage on spring 2 and mass damage on disk 1. Again, the true severities of stiffness damage are unknown in advance. The identified stiffness and mass parameters clearly indicates that variations of parameter are individually identified regardless of other damage type. For instance, *S1J1* increases the stiffness value of spring 1 alone, while *S2J2* only reduce the inertia for mass 2. Thus, identification of each parameter is not affected by the presence of different type of damage. Similar to the result of homogeneous damage case (Figure 2), the identified mass parameters are more consistent than stiffness parameters.

Table 1. Experimentally identified stiffness k_i, mass J_i, and damping c_i for healthy and damaged cases (all in suitable units). The bold number indicates the identified parameters of damaged one.

Parameters	Healthy	Damage Cases			
		S1	*S2*	*J1*	*J2*
k_1	2.8228	**2.9421**	2.7931	2.7350	2.7022
k_2	2.7606	2.7726	**2.8369**	2.6631	2.5940
J_1	0.0212	0.0212	0.0211	**0.0169**	0.0207
J_2	0.0203	0.0203	0.0200	0.0197	**0.0158**
c_1	0.0163	0.0156	0.0159	0.0138	0.0167
c_2	0.0062	0.0065	0.0068	0.0069	0.0059

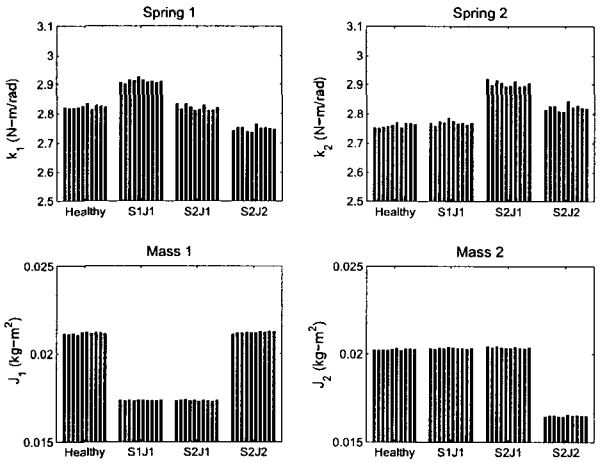

Figure 3. Experimentally identified stiffness and mass moment of inertia for healthy and three mixed damage cases: *S1J1*, *S2J1*, and *S2J2*.

It is well known that mass and stiffness changes associated with certain extent and location may produce no natural frequency shift at all due to canceling effects, which make it difficult to detect damage using only frequency-domain measurements. Thus, direct reconstruction of stiffness and mass matrices has advantage over other modal-based methods especially when the type of damage is unknown. In this regard, the

torsional plant provides a perfect exemplary apparatus for demonstrating damage detection capability, i.e., differentiating damage types in a structure. The torsional system can accommodate various type and condition of parameter perturbations without imposing interference between them. This experiment shows that mass and stiffness can be independently identified regardless of locations and amount of their changes. The identified damping parameters exhibit somewhat contrasting results. The damping parameters are not significantly affected by stiffness and mass changes except for the *Damping 1* in the mass damage cases (*J1*, *J2*, and *J12*) as shown in Figure 4. While damping is not generally considered as a damage-sensitive parameter, it is obvious that damping is more closely coupled with mass change in this experiment.

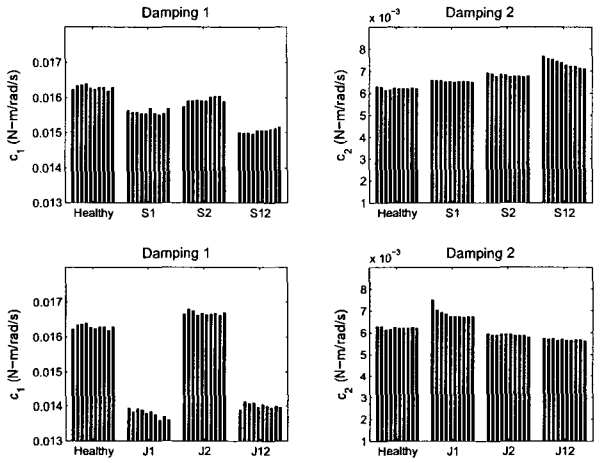

Figure 4. Experimentally identified damping parameters for healthy and six different damage cases: *S1*, *S2*, *S12*, *J1*, *J2*, and *J12*.

5. Conclusions

This experimental study has shown that direct identification of stiffness and mass matrices from input-output data provides a potential tool for structural damage detection. The KP method does not require initial finite element model or frequency-domain data. The method offers a linear solution in extracting mass, damping and stiffness matrices from realized state-space model without solving an eigenvalue problem. This experimental validation of KP method allows us to envision potential solutions for more general inverse vibration problems. The significance of this study can be found from the experimental application of newly developed system identification technique to the practical problem of structural health monitoring without given any priori information of the structure. Moreover, the presence, location, extent, and even types of damage can be directly identified.

6. Acknowledgments

The authors wish to thank Prof. Laura Ray for helpful discussions on the use of the experiment data reported in this paper. The authors also acknowledge the support of the *Texas Institute for the Intelligent Bio-Nano Materials and Structure for Aerospace Vehicles*, funded by NASA Cooperative Agreement No. NCC-1-02038.

References

[1] Juang, J.-N., Phan, M.Q., Horta, L.G., and Longman, R.W., "Identification of Observer/Kalman Filter Markov parameters: Theory and experiments," *Journal of Guidance, Control, and Dynamics*, Vol. 16, No. 2, 1993, pp. 320-329.

[2] Juang, J.-N., and Pappa, R.S., "An eigensystem realization algorithm for model parameter identification and model reduction," *Journal of Guidance, Control, and Dynamics*, Vol. 8, No. 5, 1985, pp. 620-627.

[3] Alvin, K.F., and Park, K.C., "Second-order structural identification procedure via state-space-based system identification", *AIAA Journal*, Vol. 32, No. 2, 1994, pp. 397-406.

[4] Tseng, D.H., Longman, R.W., and Juang, J.-N., "Identification of gyroscopic and nongyroscopic second-order mechanical systems including repeated roots problems," *Advances in Astronautical Sciences*, Vol. 87, AAS 94-151, 1994, pp. 145-165.

[5] Angelis D., Lus, H., Betti, R., and Longman, R.W., "Extracting physical parameters of mechanical models from identified state space representations," *ASME Journal of Applied Mechanics*, Vol. 69, September, 2002, pp. 617-625.

[6] Phan, M.Q., and Longman, R.W., "Extracting mass, stiffness, and damping matrices from identified state-space models," Paper AIAA-2004-5415, *AIAA Conference on Guidance, Navigation, and Control*, Providence, RI, August 16-19, 2004.

[7] Ray, L.R., and Koh, B.H., "Enhancing Uniqueness Properties in Damage Identification using Sensitivity Enhancing Control," *Materials Evaluation*, Vol. 61, No. 10, 2003, pp. 1134-1142.

[8] Koh, B.H., "Damage identification of smart structures through sensitivity enhancing control," *Doctoral Dissertation, Thayer School of Engineering, Dartmouth College*, New Hampshire, March, 2003.

[9] Parks, T.R., "Manual for Model 205/205a: Torsional Control System," *EPC Educational Control Products*, Woodland Hills, California, 91367, 1999.